Research Square

Preprints are preliminary reports that have not undergone peer review.
They should not be considered conclusive, used to inform clinical practice,
or referenced by the media as validated information.

S100PBP is regulated by mutated KRAS and plays a tumour suppressor role in pancreatic cancer

Kirtiman Srivastava (kirtiman.srivastava@ucb.com)
Barts Cancer Institute
Kate Lines
University of Oxford
Daria Jach
Barts Cancer Institute
Tatjana Crnogorac-Jurcevic
Barts Cancer Institute, QMUL https://orcid.org/0000-0002-2465-5605

Article

Keywords: S100PBP, S100P, p53, RhoB, AKT, KRAS, MS-275

Posted Date: April 18th, 2023

DOI: https://doi.org/10.21203/rs.3.rs-2731268/v1

License: This work is licensed under a Creative Commons Attribution 4.0 International License.
Read Full License

Version of Record: A version of this preprint was published at Oncogene on October 4th, 2023. See the published version at https://doi.org/10.1038/s41388-023-02851-y.

Abstract

We have previously shown that expression of S100PBP, an S100P binding partner, gradually decreases during progression of pancreatic ductal adenocarcinomas (PDAC). Here, we show that loss of S100PBP leads to oncogenic transformation of pancreatic cells; after deregulation of *S100PBP* expression, both *in silico* and *in vitro* analyses highlighted alterations of genes known to modulate cytoskeleton, cell motility and survival. Overexpression of S100P reduced S100PBP expression, while co-immunoprecipitation indicated the interaction of S100P with S100PBP-p53-ubiquitin protein complex, likely causing S100PBP degradation. The doxycycline-induced $Kras^{G12D}$ activation resulted in decreased S100PBP levels, while low-dose treatment with HDAC inhibitor MS-275 rescued its expression in both human and mouse PDAC cell lines. This indicates $Kras^{G12D}$ as an upstream epigenetic regulator of S100PBP. Finally, analysis of TCGA PanCancer Atlas PDAC datasets demonstrated poor prognosis in patients with high *S100P* and low *S100PBP* expression, suggesting that S100PBP is a novel tumour suppressor gene with potential clinical utility.

Introduction

We have previously discovered a novel interacting partner of small Ca^{2+}-binding S100P protein, S100PBP (S100P-binding protein) (1), which is almost ubiquitously expressed and shows no homology to any currently known protein. We have also demonstrated that silencing or overexpression of S100PBP leads to increase and decrease of cathepsin Z (*CTSZ*), respectively, and that S100PBP mediates cell adhesion by CTSZ/$\alpha_v\beta_5$ integrin-specific interaction (2). Very few additional studies on S100PBP have been reported until now. Integrated bioinformatic analysis of our array data (2) to identify genes and pathways downstream of S100PBP in pancreatic cancer (3) showed its role in miRNA signaling, in cytoskeletal anchoring and protein binding activity, as well as its role in inhibiting migration and invasion. The second report shows S100PBP to be one of the targets of *miR-944*, which is located in the intron of tumour protein p63 gene (*TP63*) and promotes cell proliferation, migration and invasion in cervical cancer (4). Finally, genome-wide scanning of copy number alterations identified *S100PBP* as one of the genes in three-gene signature which proved to be a reliable biomarker to predict relapse-free survival in post-hepatectomy patients with colorectal cancer liver metastases (5). However, no other information about this protein is available, and detailed functional roles of S100PBP are currently completely unknown.

In pancreas, S100PBP is expressed in both exocrine and endocrine compartments (1, 2), and is largely confined to the nucleus. However, in pancreatic intraepithelial neoplasia (PanIN), a precursor lesions to pancreatic ductal adenocarcinoma (PDAC), it was either expressed in the cytoplasm or was lost. This gradual loss of S100PBP expression during PDAC progression was in stark contrast to increasing levels of pro-oncogenic S100P protein (1, 2). Given that S100P overexpression is linked with cytoskeletal remodelling and increased motility and invasion (6), we hypothesised that S100PBP could also be implicated in their physiological regulation.

In this study, we therefore aimed to unravel the detailed roles of S100PBP, its interactions with effector molecules which may modulate cell morphology, motility and invasion, and cell survival, all of which could corroborate its potential role of novel tumour suppressor.

Material And Methods

Tissue culture

Cell lines from human PDAC (CFPac1, Panc1, MIA PaCa2, PaTu-8988s/t), human chronic myeloid leukaemia (CML; HAP1-parental and HAP1-CRISPR-Cas9 S100PBP knockout cells purchased from Horizon Discovery, UK) and doxycycline-inducible $Kras^{G12D}$ mouse PDAC cell lines (7) were cultured in their respective media with 10% FBS and Pen/Strep in humidified tissue culture incubators. The mouse PDAC cell lines were treated with doxycycline (100µg/mL) for 48 hours before protein and RNA analysis. The identity of all the cell lines used were verified by short tandem repeat profiling. The phase contrast images of these cells were captured using 10X magnification on light microscope (Olympus, Germany).

Western Blotting

The differential protein expressions between cell lines with differing levels of S100PBP expression, and after S100PBP gene manipulation were studied as described previously (8). Briefly, 50µg whole cell lysate was resolved by SDS-PAGE using 7.5%-15% polyacrylamide gels before blotting onto nitro cellulose membrane (0.2µm pore size, GE Health Sciences, UK). The target proteins were detected by antibodies listed in Supplementary table 1), and visualised by chemi-luminescence substrate (Millipore, UK).

Real-time PCR

qPCR was conducted as previously described(8). Briefly, the total RNA was harvested from cell pellets by Tripure reagent (Roche, USA) before quantification. 2µg of RNA was used for single strand synthesis by single strand synthesis kit (Roche, USA) before setting qPCR reaction using primers detailed in Supplementary table 2 and SYBr green reagent (Applied Biosciences, UK) on ABI 7500 real-time machine (Applied Biosciences, UK).

Immunofluorescence

The cellular localisation of filamentous Actin (F-actin) was conducted by detection and visualisation of Rhodamine-labelled phalloidin (Life Technologies, UK) as previously described (9). The other cellular proteins were visualised using LSM710 confocal microscope (Zeiss, Germany) as described previously (8, 10).

Cell migration and invasion assays

The relative rate of cell migration was studied by culturing the cells ($0.5x10^6$) in 2D on collagen-I coated 6-well tissue culture plates before treatment with mitomycin C (2µg/mL) for 2 hours and creation of similar size scratch wounds as previously described(10). The cell motility and wound closure were

recorded by capturing scratch wound images using 10X magnification on time-lapsed microscope (Axio-Vision, UK) kept in humidified tissue culture cabinet. For 2D cell invasion assays, the cells ($5x10^4$) suspended in serum-free DMEM were seeded on Matrigel-coated transwell inserts (0.8µm pore size) kept in 24-well tissue culture plates before their incubation for 48 hours. The cells which passed through the pores were fixed in 100% methanol before their visualisation by Giemsa blue staining. The cells were counted from five representative images/insert captured by 20X magnification on light microscope (Olympus, Germany).

Transient gene silencing

50nM siRNA was used to silence S100PBP in cells (Panc1 and MIA PaCa2). Briefly, $0.5x10^6$ cells were seeded in tissue culture dishes before treatment with either scram (non-target) or two independent siRNA molecules against human S100PBP (Mol1: AUGGUGGUUCACACAAG

UCAA, Mol2: CUGUGUGAGUAAUGCAUUCUA; Qiagen, UK) mixed with RNAiMax transfection reagent (Life Technologies, UK). Fresh medium was replaced after 16 hours, and cells were harvested for protein and RNA analysis after 72 hours of transfection. A fraction of cells from matching population were cultured on glass coverslips in their respective medium for cellular localisation studies.

Stable gene over-expression

The stable expression of S100PBP was conducted in low S100PBP-expressing cells (CFPac1 and PaTu-8988t) by using expression vector pCMV-Tag2B carrying full length S100PBP gene and matching empty vector (EV) as previously described (1, 2). Similarly, the Panc1 cell lines with stable expression of S100P were established using pcDNA3.1 carrying full length S100P. Briefly, cells ($0.2x10^6$/well) seeded in 6-well tissue culture plates were treated with a mixture of plasmid and FuGene6 transfection (Promega, UK) reagent for 48 hours. The transfected cells were selected by treatment with 1.1mg/mL geneticin (G418 sulphate) antibiotic (InvivoGen, UK) for three weeks. The mRNA and protein analyses were conducted to confirm the stable expression of genes in the respective cell lines.

Co-immunoprecipitation

The protein-protein interactions were studied by co-immunoprecipitaion. Briefly, 4µg rabbit polyclonal antibodies (anti-S100PBP and IgG) were crosslinked with protein G-tagged Dynabeads (Life Technologies, UK) according to the manufacturer's instructions. The antibody- Dynabeads complexes were incubated with the whole cell lysates ($15x10^6$ cells lysed in NP-40 buffer) under constant rotation for 24 hours at 4 C. A magnet was used to separate antigen-antibody-Dynabeads complex from the lysates, before non-denaturing elution of antibody- antigen complex. Laemmli buffer (Sigma-Aldrich, UK) was added to the eluted sample and input (2% whole cell lysate) sample before visualising proteins by Western blotting.

In silico **analysis**

The Affymetrix gene expression profiling was conducted using RNA isolated from MIA PaCa-2 and FA6 cells after deregulation of S100PBP expression as described previously (2). These data have been deposited to the National Center for Biotechnology Information's Gene Expression Omnibus (http://www.ncbi.nlm.nih.gov/geo, accession number GSE35199).

The generated datasets were analysed using Ingenuity Pathway Analysis (IPA)(Qiagen, UK) to build networks of inter-linked signalling molecules. The Cancer Genome Atlas (TCGA) PanCancer Atlas datasets for PDAC (n = 177) were used to conduct analysis using the cBioPortal for cancer genomics website (https://www.cbioportal.org/) and the Protein Atlas website (https://www.proteinatlas.org/).

Flow cytometry

The quantification of cells undergoing apoptosis was conducted by FITC Annexin V apoptotic detection assay kit (BD Biosciences, USA). Briefly, 10^5 cells/well were seeded on collagen-I coated 6-well plates before 72 hours treatment with gemcitabine (0.01µM). The medium and trypsinised cells were centrifuged at 500g for 5 minutes (ThermoScientific, UK) to form cell pellets, which were resuspended in 1x binding buffer containing FITC-labelled annexin V and propidium iodide (PI). The early and late apoptosis detection was conducted by flow cytometer LSR Fortesa-3 and analysed by FACS DIVA software (BD Biosciences, USA).

Statistical analysis

All experiments were performed three times unless indicated otherwise. Data are presented as mean ± SD. Statistical analysis was performed using student's *t*-test and one-way analysis of variance (ANOVA) followed by Dunnet's post hoc analysis where more than 2 groups were compared; GraphPad Prism v8 software was utilised. The $P < 0.05$ was considered to be significant in all experiments.

Results

A role of S100PBP in cell morphology, motility and invasion

In silico IPA analysis of our previous transcriptome data of MIA PaCa-2 and FA6 PDAC cell lines after silencing and overexpressing *S100PBP*(2) highlighted the involvement of several signalling networks known to modulate cell morphology, motility and survival, such as RhoB, p53 and AKT signalling (Fig. 1a, b). This was verified *in vitro* in CML and several PDAC cell lines: the S100PBP protein was highly expressed in Panc1, MIA PaCa-2 and HAP1-parental cells, which also showed elevated expression of RhoB, p-myosin phosphatase1 (MYPT1)-S^{696} and p-cofilin-S^3, indicating an active RhoB/Rho-kinase (ROCK) signalling (Fig. 1c). In contrast, the cells expressing low levels of S100PBP (CFPac1, PaTu-8988s/t) and HAP1-S100PBP knockout cells showed low levels of these proteins (Fig. 1c), indicating the potential regulatory role of S100PBP in RhoB/ROCK signalling. This was also supported by cellular localisation of F-actin, with an intense F-actin presence in cortical area, alongside presence of stress fibres in cells with high S100PBP, while diminished F-actin cortical staining and loss of stress fibres were

observed in cells expressing low or no S100PBP expression (Fig. 1d). Interestingly, this cytoskeletal rearrangement which correlated with S100PBP expression status was also manifested in distinct cellular morphology: while cells expressing high levels of S100PBP appeared to have cobblestone-like polygonal shape with well-defined morphology, the cells expressing low S100PBP appeared to have spindle, elongated shape with poorly defined morphology **(Supplementary Fig. 1a)**.

To further confirm that S100PBP status governs the stability of cytoskeleton, we silenced S100PBP using two independent siRNA molecules (siRNA mol1 and 2) in S100PBP-expressing Panc1 and MIA PaCa-2 cells. This led to lower expression and activity of RhoB marked by low levels of RhoB, p-MYPT1-S^{696} and p-cofilin-S^{3} in S100PBP silenced groups compared to scram (non-target) siRNA-treated control group (Fig. 2a). The low level of RhoB mRNA in HAP1-S100PBP knockout cells and Panc1 cells after transient S100PBP silencing indicates the S100PBP-mediated transcriptional modulation of RhoB **(Supplementary Fig. 2a, b**, third panel**)**. The localisation of F-actin in Panc1 and MIA PaCa-2 cells after S100PBP silencing was further supportive of these results, with intense F-actin cortical staining alongside stress fibre formations in the control cells, and a weak F-actin cortical staining with loss of stress fibres in S100PBP-silenced cells (Fig. 2b). Similar F-actin distribution in HAP1 cells after S100PBP gene knockout was also shown (Fig. 1d).

We next assessed the functional significance of silencing S100PBP in Panc1 and MIA PaCa-2 cells (only siRNA mol2 was used). The 2D scratch wound assay and time-lapse microscopy demonstrated that S100PBP silencing significantly enhanced the rate of cell migration (Fig. 2c), showing that S100PBP-induced morphological changes are accompanied by changes in cellular motility. Furthermore, S100PBP-silenced MIA PaCa-2 cells also showed significantly higher number of cells invading the Matrigel-coated inserts compared to their matching controls (Fig. 2d); increased invasive capabilities of Panc1 cells after S100PBP silencing we already reported on previously (2). Thus, silencing of S100PBP potentiated the cell motility and invasion capabilities.

To further ascertain the roles of S100PBP in regulation of cell morphology, motility and invasion, we generated stable S100PBP over-expressing cell lines CFPac1 and PaTu-8988t, which endogenously express low levels of S100PBP (Fig. 3a and **Supplementary Fig. 3a**). Such engineered cells expressed high levels of RhoB protein (Fig. 3a) which coincided with their distinct round, compact, cobblestone-like polygonal morphology compared to the empty vector (EV) control cells, which retained elongated shape and spindle morphology **(Supplementary Fig. 1b)**. In addition, the high S100PBP expressing population showed a significantly lower rate of both cell migration and invasion (Fig. 3b and 3c). Taken together, these results confirm the role of S100PBP in (negative) regulation of motility invasion.

S100PBP interacts with p53 and is involved in apoptosis regulation via AKT signalling

IPA highlighted *TP53* and *AKT* as additional effector genes involved in cell movement after deregulation of *S100PBP* (Fig. 1a). Interestingly, the endogenous levels of p53 in PDAC and HAP1 cells mirrored the

pattern of their S100PBP expression (Fig. 4a). Furthermore, the transient S100PBP gene silencing in Panc1 and MIA PaCa-2 cells reduced both the mRNA and protein levels of p53 (Fig. 4b and **Supplementary Fig. 2b**, middle panel), thus indicating the involvement of S100PBP in modulation of p53 expression. As several S100 proteins bind to and interact with p53(11, 12), we wanted to establish if p53 also interacts with S100PBP. Indeed, the co-immunoprecipitation studies using whole cell lysates of Panc1 and MIA PaCa-2 cells indicated that these two proteins can also interact (Fig. 4c). In these two cell lines, p53 was shown to be confined to the nucleus (the intense nuclear localisation of p53 was also observed in S100PBP-expressing CFPac1, **Supplementary Fig. 4a**), suggesting that this is where S100PBP and p53 interact (Fig. 4d).

We next studied the potential role of S100PBP in modulation of AKT signalling as suggested in Fig. 1b. We observed the activation of AKT pathway, marked by upregulation of p-AKT-S^{473} in cells with low S100PBP expression (Fig. 5a). Consistent with these results, the transient silencing of S100PBP expression in Panc1 and MIA PaCa-2 cells decreased the levels of p53 (Fig. 4b) and its transcriptional target, pro-apoptotic PUMAα/β, while activating AKT and upregulating anti-apoptotic Bcl-2 protein (Fig. 5b). Since Ki67 levels remained unaffected in these cells, the activation of pro-survival AKT signalling appeared to be independent of its cell proliferation role (Fig. 5b and **Supplementary Fig. 4a)**. The functional significance of AKT activation was studied by FITC-Annexin V flow cytometry after silencing S100PBP in Panc1 and MIA PaCa-2 cells, before treating these cells and their respective controls (Scram) with gemcitabine (0.01µM) for 96 hours. The significant reduction in the percentage of apoptotic cells in the S100PBP-silenced population is shown on Fig. 5c, implicating S100PBP in apoptotic modulation via AKT signalling. Using PDAC cells with ectopic expression of S100PBP, we further observed that cells with high S100PBP expression also expressed elevated levels of p53 protein, while alleviating pAKT-S^{473} levels (Fig. 6a). The pro-survival role of S100PBP was further confirmed by treating the control CFPac1 and PaTu-8988t cells and their S100PBP-expressing counterparts with 0.01µM gemcitabine for 96 hours. The flow cytometry data indicated significant increase in the percentage of apoptotic cells with high S100PBP levels (Fig. 6b). The overactivity of pro-apoptotic caspase-3, marked by high levels of cleaved caspase-3 and presence of cleaved PARP seen in these cells further suggested the role of S100PBP in increased chemosensitivity **(Supplementary Fig. 4b)**.

Given that several S100 proteins, including S100P, play a pivotal role in posttranslational modification, stabilisation and cellular trafficking of p53 (12, 13) and that the expression of S100P increases with concomitant depletion of S100PBP during PDAC development(2), we investigated the role of S100P in modulating S100PBP expression. Similarly to what we have shown previously in histological analysis, Western blot data showed that the high S100PBP-expressing cells Panc1 and MIA PaCa-2 express low levels of S100P, in contrast to CFPac1 cells with high S100P expression (Fig. 6c). To further investigate this, we established three Panc1 cell lines with stable expression of S100P: Line 1 and 2 had high levels, and Line 3 low levels of S100P (Fig. 6d). Analysis of these three cell lines and EV control Panc1 cells showed low levels of S100PBP, p53, PUMAα/β and RhoB, and activated AKT in the Lines 1 and 2 (Fig. 6d). Interestingly, the cell lines stably expressing S100P showed distinct morphological changes:

while the control cells exhibited cuboidal shape with cobblestone-like morphology, Panc1 lines 1 and 2 with high S100P showed elongated shape and spindle morphology **(Supplementary Fig. 1c)**. Interestingly, the S100PBP transcript expression in these cells did not change significantly, suggesting that changes in protein levels were not due to transcriptional regulation **(Supplementary Fig. 5**, two upper panels**)**. Panc1 line 3, which expresses low levels of S100P and high level of S100PBP protein **(**Fig. 6d**)** was utilised for the immunoprecipitation experiments, which confirmed the S100PBP-p53 protein interaction observed earlier. Furthermore, additional co-immunoprecipitation of S100P and ubiquitin in the same sample and their presence in S100PBP-p53 complex **(**Fig. 6e**)** potentially indicated the targeting of S100PBP and/or p53 for degradation. This suggests that the interaction of S100P and S100PBP (and p53) is highly dynamic and transient, and could explain somewhat counteractive finding of inverse expression of S100P and S100PBP in cells *in vitro* and in tissue sections, as reported previously (1, 2).

The functional significance of the AKT activation in Panc1 cells expressing high S100P levels was studied by treating control and line 1 cells with 0.01µM gemcitabine for 96 hours followed by FITC-Annexin V apoptotic assay. The results indicated a significant reduction in percentage of apoptotic line 1 cells compared to the control population **(**Fig. 6f**)**, confirming the role of S100P in enhancing chemoresistance.

Kras^{G12D} regulates S100PBP via epigenetic mechanism

Mutant *KRAS* is known regulator of various S100 proteins in many cancers (14, 15), and is an earliest driver of PDAC development; we thus wanted to establish if mutant *KRAS* plays a role in modulating the expression of S100PBP, especially since total KRAS levels remained largely unchanged after stable expression of S100PBP in CFPac1 and PaTu-8988t cells **(Supplementary Fig. 3b)**. We utilised doxycycline-inducible Kras^{G12D} PDAC mouse cell lines (*iKras^{G12D}p53$^{L/+}$*)(7) to study the effects of persistent activation of mutant *KRAS* on S100PBP expression. Kras^{G12D} activation resulted in downregulation of S100PBP **(**Fig. 7a**)**. In addition, upon Kras^{G12D} activation, the translocation of S100PBP to the cytoplasm was seen **(**Fig. 7b**)**, mimicking the data we observed in human PanIN lesions (1, 2). Taken together, these results suggest the upstream regulatory role of mutated Kras^{G12D} on S100PBP.

We further show that Kras^{G12D} activation also decreased the levels of RhoB, p-MYPT1-S^{696} and p-cofilin-S^{3}, thereby indicating attenuated RhoB signalling axis **(**Fig. 7a**)**. Furthermore, weak and disrupted F-actin cortical staining was also seen after Kras^{G12D} activation, which showed intense F-actin cortical presence along with stress fibre formations traversing across the cell surface **(**Fig. 7c**)**. With reorganisation of the cytoskeleton, Kras^{G12D} activation also resulted in altered cellular morphology from round and cobblestone-like shape in control population to elongated and spindle shape in Kras^{G12D}-activated population **(Supplementary Fig. 1d)**. Finally, Kras^{G12D} activation also led to the depletion of p53 and PUMAα/β proteins, while increasing Bcl-2 levels and activated pro-survival AKT signalling **(**Fig. 7a**)**. Taken together, these results substantiated S100PBP as a downstream target of mutated Kras^{G12D}, indicating that its loss could be pivotal for PDAC development and progression.

Since the over-activity of class-I histone deacetylases (HDACs) modulated by mutant KRAS has been reported in PDAC previously (16, 17), and HDAC was also highlighted in our IPA signalling network shown on Fig. 1b, we tested the potential role of HDAC in regulation of S100PBP expression. The treatment of CFPac1 and PaTu-8988t cells with low doses of class-I HDAC inhibitor, MS-275/Entinostat(18), rescued the expression of S100PBP and acetyl histone H3 in a dose dependent manner (Fig. 8a). Additionally, the pre-treatment of $Kras^{G12D}$ PDAC mouse cell line-A with 0.2μM MS-275 also increased the levels of S100PBP and acetyl lysine (Fig. 8b). While doxycycline-mediated activation of $Kras^{G12D}$ suppressed S100PBP, pre-treatment with 0.2μM MS-275 largely abated the effects of $Kras^{G12D}$ overactivation by rescuing and maintaining S100PBP levels similar to untreated controls (Fig. 8b). These results indicate that $Kras^{G12D}$-mediated regulation of S100PBP is, at least partially, modulated via epigenetic mechanism.

High expression of S100P and low expression of S100PBP correlate with poor prognosis

Finally, to establish the potential clinical relevance of *S100P* and *S100PBP*, we studied TCGA PanCancer Atlas dataset on 176 pancreatic adenocarcinoma patients and generated Kaplan-Meier survival plots (Fig. 8c). It is evident that patients with high *S100P* and low *S100PBP* expression have decreased survival.

Discussion

In this study we report novel tumour suppressive functions of S100PBP, including modulation of cytoskeletal reorganisation, cell morphology, motility and invasion. We show that the underlying mechanisms involve a small GTP-binding protein RhoB and its effector Rho-kinase (ROCK)-1/2 (proxies for this being phosphorylated levels of MYPT-1 and cofilin proteins seen in our data), which are well known to balance the stabilisation/destabilisation of filamentous (F)-actin and modulate the cytoskeleton-dependent processes such as cell shape and motility (19, 20). We have previously observed deregulation of p-cofolin-S^3, which inhibits actin polymerisation and cortical F-actin localisation after overexpression of S100P in PDAC cells (6). We have now expanded the study to its binding partner, S100PBP, and demonstrate distinct changes in the F-actin profile marked by the disappearance of stress fibres and/or weak F-actin cortical presence in cells endogenously expressing low S100PBP or after S100PBP gene silencing. Similar morphological changes, alongside enhanced motility and invasion in cells with low F-actin polymerisation and cortical presence have been described previously (21, 22, 23). As these changes match the pattern of RhoB expression and activity - downregulation of RhoB promotes cell migration and invasive behaviour (24, 25), and we demonstrate a direct correlation between RhoB and S100PBP expression in both PDAC and CML cells. This data indicate that S100PBP plays an important role in modulating cytoskeleton, cell morphology, motility and invasion via RhoB signalling.

Unlike other members of Rho family, like RhoA and RhoC, which play oncogenic roles (20, 26), RhoB has been shown to suppress tumorigenesis in pancreatic and other cancers (24, 27, 28, 29). Furthermore, in

RhoB-deficient mice the number of Ras-induced tumours increased compared to wt-mice (30), and loss of RhoB led to increased metastatic dissemination of lung cancer cells, which was mediated by AKT (24). This was further substantiated in study by Jiang et al, who showed that oncogenic Ras downregulates RhoB expression by a PI3K/AKT signalling (31). Finally, low RhoB expression in human PDAC samples (27), which mimics the behaviour of S100PBP described in our previous study (2), firmly implicates S100PBP in the same RhoB signalling circuitry and suggests its tumour suppressive functions.

The role of p53 in modulating cell morphology and motility by supressing cell polarisation, formation of protrusions and spreading was shown previously (32, 33, 34, 35). In addition, several studies have demonstrated the role of p53 in suppressing cell migration and metastasis (36, 37). Interestingly, these 'atypical' roles of p53 are largely mediated via controlling actin cytoskeletal organisation through Rho signalling (38, 39), which is corroborated by data in the present study. In PDAC, p53 is a well-known tumour suppressor: a loss of its functions is critical in dysregulation of cell cycle checkpoints and apoptosis, resulting in acceleration of PDAC progression and metastatic formation in both mouse models of PDAC as well as in pancreatic cancer patients (7, 40, 41, 42, 43).

Interestingly, our data suggest that S100PBP both regulated *TP53* at the transcription level, and also interacted with p53 in the nucleus. S100P and several other members of S100 family were previously shown to bind to p53 and interfere with its oligomerisation, stabilisation and cellular trafficking, thus regulating its activity (11, 12, 13). We now demonstrate for the first time that S100PBP also binds to p53, and show the existence of S100PBP-p53-S100P-ub protein complex, which could be pivotal in destabilisation and/or degradation of both S100PBP and p53. While further experiments are needed to delineate the ubiquitination pathway and proteasomal degradation machinery regulating the stability of these two proteins, it is tempting to speculate that (as suggested by loss of S100PBP in PanIN progression seen in histological analysis of PDAC tissues) this is also happening *in vivo* during PDAC development. Loss of S100PBP would 'free' S100P, a highly invasive protein, which will abrogate p53 function, leading to early metastatic spread of PDAC cells.

Loss of p53 expression is known to accompany elevated levels of endogenous PI3K (phosphoinositide 3-kinase) and AKT activity (38, 44). This AKT overactivation has a major role in growth signal autonomy, inhibition of apoptosis and chemoresistance, and is frequently disturbed in many cancer types (45, 46). In PDAC, AKT is overexpressed by 50%, and its overexpression is well known to be a negative prognostic factor (47, 48). We observed an inverse correlation between AKT activation (proxy being pAKT-S^{473} levels) and S100PBP expression in both PDAC and CML cells. The ectopic expression of S100PBP in PDAC cells decreased AKT activation and chemoresistance to gemcitabine, suggesting the presence of AKT-mediated intrinsic chemoresistance seen previously (49), now also in PDAC cells with low S100PBP expression.

Given that activating mutations in *KRAS* are initial drivers of PDAC, we hypothesised that they may also directly or indirectly affect the S100PBP signalling. Indeed, $Kras^{G12D}$ activation in mouse cell lines from inducible oncogenic *KRAS* model of PDAC (7) led to downregulation of S100PBP protein and triggered its

nuclear-to-cytoplasmic translocation. In addition, the downstream effects of $Kras^{G12D}$ activation on RhoB, AKT and p53 signalling axes mirrored the *in vitro* data obtained after S100PBP silencing and thus provided mechanistic evidence of KRAS as an upstream regulator of S100PBP signalling axes, as illustrated in Fig. 8d.

Several studies in various cancers, including pancreatic, have also indicated the role of overactivated *KRAS* in supressing the pro-apoptotic and tumour suppressor genes by enhancing the epigenetic modifications of histones (50, 51, 52, 53). The elevated expression and activity of class-I HDACs have been previously reported in PDAC (16, 54). We here show that the treatment with a class-I specific HDAC inhibitor MS-275 rescued the expression of S100PBP *in vitro* by, at least partially, attenuating the $Kras^{G12D}$-evoked suppression of S100PBP. This demonstrates a role of epigenetic mechanism in S100PBP regulation, as shown previously for S100P(55). HDAC inhibitors like vorinostat have shown promising outcomes by augmenting cell death and supressing advanced pancreatic (and other) cancers (50, 52, 53, 56), and our data now implicate S100PBP in the mechanisms of their actions. Further studies with individual members of class-I HDACs, which may have a direct or indirect role in the epigenetic regulation of S100PBP and exert potential therapeutic benefit, are now warranted.

Taken together, in the present study we demonstrate a novel tumour suppressive role of S100PBP via its regulation of cellular morphology, motility, invasion and pro-survival capabilities. We implicate S100PBP as a novel intermediate and a critical signalling molecule in Kras/AKT/RhoB/p53 signalling axes and suggest its epigenetic regulation. Given that the high expression of *S100P* and low expression of *S100PBP* correlate with poor survival in PDAC patients, this study highlights the potential clinical relevance of S100PBP in pancreatic cancer.

Declarations

Acknowledgement

The inducible iKras PDAC mouse model was generated by Prof. Ronald DePinho's Laboratory (MD Anderson Cancer Center, Houston, TX), and the iKras PDAC cell-lines isolated from this model were a gift from Dr. Faraz Mardakheh (Barts Cancer Institute). The authors would also like to thank Flow cytometry Core facility team at Barts Cancer Institute for the training and support provided towards this study.

Author contribution

KS and TCJ designed the study and wrote the manuscript. KS, DJ and KL generated the data.

Competing interests

The authors declare no potential conflicts of interest.

Data availability statement

The data generated during and/or analysed during the current study are available from the corresponding author on reasonable request.

References

1. Dowen SE, Crnogorac-Jurcevic T, Gangeswaran R, Hansen M, Eloranta JJ, Bhakta V, et al. Expression of S100P and its novel binding partner S100PBPR in early pancreatic cancer. Am J Pathol. 2005;166:81-92.
2. Lines KE, Chelala C, Dmitrovic B, Wijesuriya N, Kocher HM, Marshall JF, et al. S100P-binding protein, S100PBP, mediates adhesion through regulation of cathepsin Z in pancreatic cancer Cells. Am J Pathol. 2012;180:1485-1494.
3. Lu YJ, Yang Y, Hu TH, Duan WM. Identification of key genes and pathways at the downstream of S100PBP in pancreatic cancer cells by integrated bioinformatical analysis. Transl Cancer Res. 2021;10:806-816.
4. Xie H, Lee L, Scicluna P, Kavak E, Larsson C, Sandberg R, et al. Novel functions and targets of miR-944 in human cervical cancer cells. Int J Cancer. 2015;136:E230-E241.
5. Yang PS, Hsu HH, Hsu TC, Chen MJ, Wang CD, Yu SL, et al. Genome-wide scan for copy number alteration association with relapse-free survival in colorectal cancer with liver metastasis patients. J Clin Med. 2018;7. Epub 20181118.
6. Whiteman HJ, Weeks ME, Dowen SE, Barry S, Timms JF, Lemoine NR, et al. The role of S100P in the invasion of pancreatic cancer cells is mediated through cytoskeletal changes and regulation of cathepsin D. Cancer Res. 2007;67:8633-8642.
7. Ying HQ, Kimmelman AC, Lyssiotis CA, Hua SJ, Chu GC, Fletcher-Sananikone E, et al. Oncogenic Kras maintains pancreatic tumors through regulation of anabolic glucose metabolism. Cell. 2012;149:656-670.
8. Srivastava K, Pickard A, Craig SG, Quinn GP, Lambe SM, James JA, et al. Delta Np63 gamma/SRC/Slug signaling axis promotes epithelial-to-mesenchymal transition in squamous cancers. Clin Cancer Res. 2018;24:3917-3927.
9. Srivastava K, Shao B, Bayraktutan U. PKC-beta exacerbates in vitro brain barrier damage in hyperglycemic settings via regulation of RhoA/Rho-kinase/MLC2 pathway. J Cereb Blood Flow Metab. 2013;33:1928-1936.
10. Srivastava K, Pickard A, McDade S, McCance DJ. p63 drives invasion in keratinocytes expressing HPV16 E6/E7 genes through regulation of Src-FAK signalling. Oncotarget. 2017;8:16202-16219.
11. van Dieck J, Fernandez-Fernandez MR, Veprintsev DB, Fersht AR. Modulation of the oligomerization state of p53 by differential binding of proteins of the S100 family to p53 monomers and tetramers. J Biol Chem. 2009;284:13804-13811.
12. Fernandez-Fernandez MR, Veprintsev DB, Fersht AR. Proteins of the S100 family regulate the oligomerization of p53 tumor suppressor. Proc Natl Acad Sci U S A. 2005;102:4735-4740.

13. Gibadulinova A, Pastorek M, Filipcik P, Radvak P, Csaderova L, Vojtesek B, et al. Cancer-associated S100P protein binds and inactivates p53, permits therapy-induced senescence and supports chemoresistance. Oncotarget. 2016;7:22508-22522.
14. Woo T, Okudela K, Mitsui H, Tajiri M, Rino Y, Ohashi K, et al. Up-regulation of S100A11 in lung adenocarcinoma-its potential relationship with cancer progression. PLoS One. 2015;10:e0142642.
15. Bydoun M, Sterea A, Liptay H, Uzans A, Huang WY, Rodrigues GJ, et al. S100A10, a novel biomarker in pancreatic ductal adenocarcinoma. Mol Oncol. 2018;12:1895-1916.
16. Cai MH, Xu XG, Yan SL, Sun Z, Ying Y, Wang BK, et al. Depletion of HDAC1, 7 and 8 by histone deacetylase inhibition confers elimination of pancreatic cancer stem cells in combination with gemcitabine. Sci Rep. 2018;8:1621
17. von Burstin J, Eser S, Paul MC, Seidler B, Brandl M, Messer M, et al. E-cadherin regulates metastasis of pancreatic cancer in vivo and is suppressed by a SNAIL/HDAC1/HDAC2 repressor complex. Gastroenterology. 2009;137:361-371.
18. Peulen O, Gonzalez A, Peixoto P, Turtoi A, Mottet D, Delvenne P, et al. The Anti-tumor effect of HDAC inhibition in a human pancreas cancer model is significantly improved by the simultaneous inhibition of cyclooxygenase 2. Plos One. 2013;8:e75102.
19. Ellenbroek SIJ, Collard JG. Rho GTPases: functions and association with cancer. Clin Exp Metastasis. 2007;24:657-672.
20. Karlsson R, Pedersen ED, Wang Z, Brakebusch C. Rho GTPase function in tumorigenesis. Biochim Biophys Acta. 2009;1796:91-98.
21. Bousquet E, Calvayrac O, Mazieres J, Lajoie-Mazenc I, Boubekeur N, Favre G, et al. RhoB loss induces Rac1-dependent mesenchymal cell invasion in lung cells through PP2A inhibition. Oncogene. 2016;35:1760-1769.
22. Wicki A, Lehembre F, Wick N, Hantusch B, Kerjaschki D, Christofori G. Tumor invasion in the absence of epithelial-mesenchymal transition: Podoplanin-mediated remodeling of the actin cytoskeleton. Cancer Cell. 2006;9:261-272.
23. Morris HT, Machesky LM. Actin cytoskeletal control during epithelial to mesenchymal transition: focus on the pancreas and intestinal tract. Br J Cancer. 2015;112:613-620.
24. Bousquet E, Mazieres J, Privat M, Rizzati V, Casanova A, Ledoux A, et al. Loss of RhoB expression promotes migration and invasion of human bronchial cells via activation of AKT1. Cancer Res. 2009;69:6092-6099.
25. Calvayrac O, Pradines A, Raymond-Letron I, Rouquette I, Bousquet E, Lauwers-Cances V, et al. RhoB determines tumor aggressiveness in a murine EGFR(L858R)-induced adenocarcinoma model and is a potential prognostic biomarker for lepidic lung cancer. Clin Cancer Res. 2014;20:6541-6550.
26. Suwa H, Ohshio G, Imamura T, Watanabe G, Arii S, Imamura M, et al. Overexpression of the RhoC gene correlates with progression of ductal adenocarcinoma of the pancreas. Br J Cancer. 1998;77:147-152.

27. Tan YG, Yin HZ, Zhang HY, Fang J, Zheng W, Li D, et al. Sp1-driven up-regulation of miR-19a decreases RhoB and promotes pancreatic cancer. Oncotarget. 2015;6:17391-17403.
28. Marlow LA, Reynolds LA, Cleland AS, Cooper SJ, Gumz ML, Kurakata S, et al. Reactivation of suppressed RhoB is a critical step for the inhibition of anaplastic thyroid cancer growth. Cancer Res. 2009;69:1536-1544.
29. Huang M, Prendergast GC. RhoB in cancer suppression. Histol Histopathol. 2006;21:213-218.
30. Liu AX, Cerniglia GJ, Bernhardt EJ, Prendergast GC. RhoB is required to mediate apoptosis in neoplastically transformed cells after DNA damage. Proc Natl Acad of Sci. U S A 2001;98:6192-6197.
31. Jiang K, Sun JZ, Cheng J, Djeu JY, Wei S, Sebti S. Akt mediates Ras downregulation of RhoB, a suppressor of transformation, invasion, and metastasis. Mol Cell Biol. 2004;24:5565-5576.
32. Roger L, Gadea G, Roux P. Control of cell migration: a tumour suppressor function for p53? Biol Cell. 2006;98:141-152.
33. Gadea G, Roger L, Anguille C, de Toledo M, Gire V, Roux P. TNF alpha induces sequential activation of Cdc42-and p38/p53-dependent pathways that antagonistically regulate filopodia formation. J Cell Sci. 2004;117:6355-6364.
34. Gadea G, Lapasset L, Gauthier-Rouviere C, Roux P. Regulation of Cdc42-mediated morpholigical effects: a novel function for p53. Embo J. 2002;21:2373-2382.
35. Alexandrova A, Ivanov A, Chumakov P, Kopnin B, Vasiliev J. Changes in p53 expression in mouse fibroblasts can modify motility and extracellular matrix organization. Oncogene. 2000;19:5826-5830.
36. Hwang CI, Matoso A, Corney DC, Flesken-Nikitin A, Korner S, Wang W, et al. Wild-type p53 controls cell motility and invasion by dual regulation of MET expression. Proc Natl Acad of Sci U S A. 2011;108:14240-14245.
37. Chen YW, Klimstra DS, Mongeau NE, Tatem JL, Boyartchuk V, Lewis BC. Loss of p53 and Ink4a/Arf cooperate in a cell autonomous fashion to induce metastasis of hepatocellular carcinoma cells. Cancer Res. 2007;67:7589-7596.
38. Guo FK, Gao Y, Wang L, Zheng Y. P19(Arf)-p53 tumor suppressor pathway regulates cell motility by suppression of phosphoinositide 3-kinase and Rac1 GTPase activities. J Biol Chem. 2003;278:14414-14419.
39. Guo FK, Zheng Y. Rho family GTPases cooperate with p53 deletion to promote primary mouse embryonic fibroblast cell invasion. Oncogene. 2004;23:5577-5585.
40. Mello SS, Valente LJ, Raj N, Seoane JA, Flowers BM, McClendon J, et al. A p53 super-tumor suppressor reveals a tumor suppressive p53-Ptpn14-Yap axis in pancreatic cancer. Cancer Cell. 2017;32:460-473.
41. Hezel AF, Kimmelman AC, Stanger BZ, Bardeesy N, DePinho RA. Genetics and biology of pancreatic ductal adenocarcinoma. Genes Dev. 2006;20:1218-1249.
42. Maitra A, Adsay NV, Argani P, Iacobuzio-Donahue C, De Marzo A, Cameron JL, et al. Multicomponent analysis of the pancreatic adenocarcinoma progression model using a pancreatic intraepithelial

neoplasia tissue microarray. Mod Pathol. 2003;16:902-912.

43. Boschman CR, Stryker S, Reddy JK, Rao MS. Expression of p53 protein in precursor lesions and adenocarcinoma of human pancreas. Am J Pathol. 1994;145:1291-1295.
44. Higuchi M, Masuyama N, Fukui Y, Suzuki A, Gotoh Y. Akt mediates Rac/Cdc42-regulated cell motility in growth factor-stimulated cells and in invasive PTEN knockout cells. Curr Biol. 2001;11:1958-1962.
45. Wheeler DL, Dunn EF, Harari PM. Understanding resistance to EGFR inhibitors-impact on future treatment strategies. Nat Rev Clin Oncolo. 2010;7:493-507.
46. Vara JAF, Casado E, de Castro J, Cejas P, Belda-Iniesta C, Gonzalez-Baron M. PI3K/Akt signalling pathway and cancer. Cancer Treat Rev. 2004;30:193-204.
47. Edling CE, Selvaggi F, Buus R, Maffucci T, Di Sebastiano P, Friess H, et al. Key role of phosphoinositide 3-Kinase class IB in pancreatic cancer. Clin Cancer Res. 2010;16:4928-4937.
48. Yamamoto S, Tomita Y, Hoshida Y, Morooka T, Nagano H, Dono K, et al. Prognostic significance of activated Akt expression in pancreatic ductal adenocarcinoma. Clin Cancer Res. 2004;10:2846-2850.
49. Wu HW, Liang ZY, Shi XH, Ren XY, Wang K, Liu TH. Intrinsic chemoresistance to gemcitabine is associated with constitutive and laminin-induced phosphorylation of FAK in pancreatic cancer cell lines. Mol Cancer. 2009;8:125.
50. Mazur PK, Herner A, Mello SS, Wirth M, Hausmann S, Sanchez-Rivera FJ, et al. Combined inhibition of BET family proteins and histone deacetylases as a potential epigenetics-based therapy for pancreatic ductal adenocarcinoma. Nat Med. 2015;21:1163-1171.
51. Mou HW, Moore J, Malonia SK, Li YX, Ozata DM, Hough S, et al. Genetic disruption of oncogenic Kras sensitizes lung cancer cells to Fas receptor-mediated apoptosis. Proc Natl Acad of Sci U S A. 2017;114:3648-3653.
52. Yamada T, Amann JM, Tanimoto A, Taniguchi H, Shukuya T, Timmers C, et al. Histone deacetylase inhibition enhances the antitumor activity of a MEK Inhibitor in lung cancer cells harboring RAS mutations. Mol Cancer Ther. 2018;17:17-25.
53. Morelli MP, Tentler JJ, Kulikowski GN, Tan AC, Bradshaw-Pierce EL, Pitts TM, et al. Preclinical activity of the rational combination of Selumetinib (AZD6244) in combination with Vorinostat in KRAS-mutant colorectal cancer models. Clin Cancer Res. 2012;18:1051-1062.
54. Mishra VK, Wegwitz F, Kosinsky RL, Sen M, Baumgartner R, Wulff T, et al. Histone deacetylase class-I inhibition promotes epithelial gene expression in pancreatic cancer cells in a BRD4-and MYC-dependent manner. Nucleic Acids Res. 2017;45:6334-6349.
55. Wang Q, Williamson M, Bott S, Brookman-Amissah N, Freeman A, Nariculam J, et al. Hypomethylation of WNT5A, CRIP1 and S100P in prostate cancer. Oncogene. 2007;26:6560-6565.
56. Ruscetti M, Dadashian EL, Guo W, Quach B, Mulholland DJ, Park JW, et al. HDAC inhibition impedes epithelial-mesenchymal plasticity and suppresses metastatic, castration-resistant prostate cancer. Oncogene. 2016;35:3781-3795.

Figures

Figure 1

A

S100PBP silencing in MiaPaca2 cells	Up-regulated	**AKT2**, ANXA1, CTNNB1, CTTN, ECT2, MAPK8, PRKAA1, SEPT9, PIK3C2A, JAK2, NF1, CTSZ, TCF7L2, APP, KIFC1, RTN4
	Down-regulated	CALR, CBX5,ERBB2, GSN, MYH10, **RHOB**, SFRP1, SKP2, PPARA, PTPN14, TP63, RAB35, CRKL, ARHGDIA
S100PBP over-expression in FA6 cells	Up-regulated	CAV1, CST6, CXCR4, DLC1, F2R FST, GBP1, HIPK2, GALS1, MCAM, MET, MMP1, **RHOB**, SKP2, S100A4, HBEGF, ADM, PRSS1/PRSS3, SNAI2, **TP53**, ICAM1, CDKN2A, JAG2, P2RY2 IL7, PKP3, STC1
	Down-regulated	CBX5, DIAPH2, DOCK1, ELF3, ID2, INHBB, LCN2, PLAC1, PTP4A3, SPP1, TFF1, TFF2, S100A9, S100P, DICER1, ITGB2, CTSZ, C3, TCF7L2, PTHLH, SERPINA5, CXCL6

B

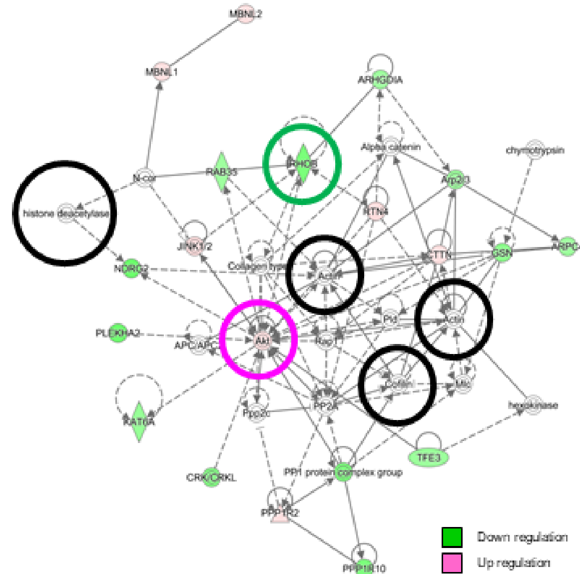

C

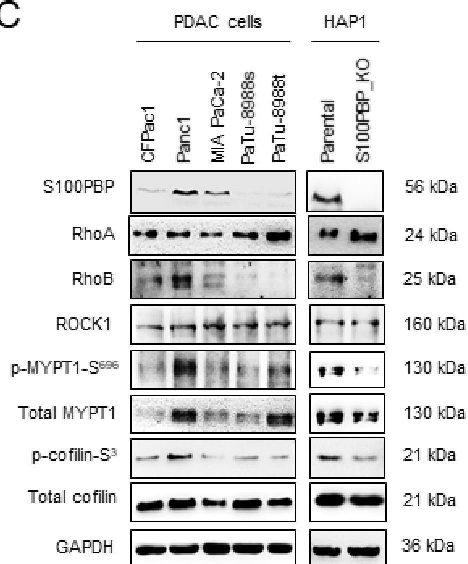

D

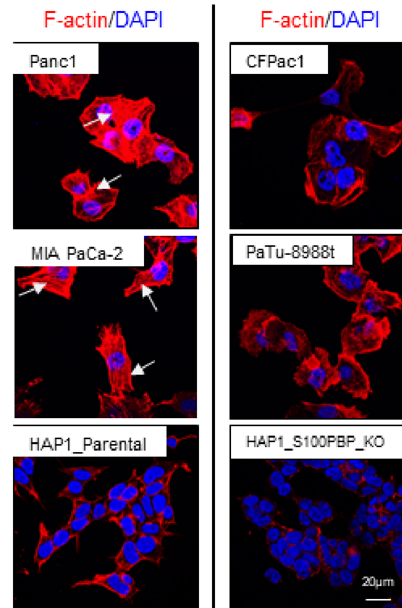

Figure 1

Network analysis highlights the role of S100PBP in modulating cellular movement. Ingenuity Pathway Analysis (IPA) of gene profiling datasets generated in MIA PaCa-2 and FA6 pancreatic cancer cell lines after deregulation of S100PBP expression: A, Filtered genes involved in cellular movement, and B, Built

relevant networks. C, Differential expression of S100PBP, RhoA, RhoB, ROCK1, p-MYPT1-S^{696}, total MYPT1, p-cofilin-S and total cofilin in panel of PDAC and HAP1 cells (parental vs S100PBP_knock out (KO). GAPDH was used as a loading control. D, Cellular localisation of F-actin in PDAC and HAP1 cell lines. Nuclei are stained by DAPI. Arrows represent stress fibre formation. Scale bar: 20µm.

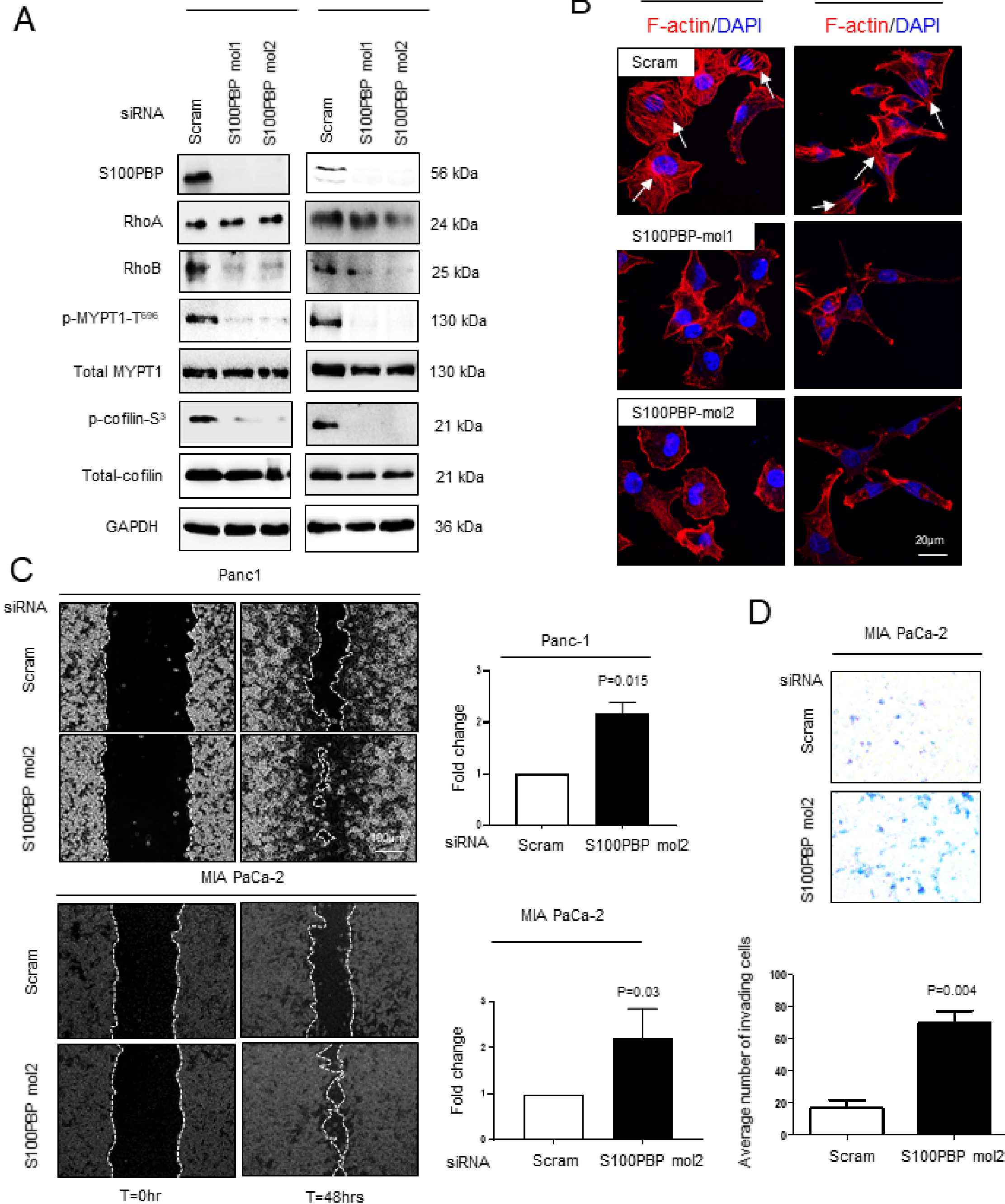

Figure 2

S100PBP silencing disrupt RhoB signalling and increases cell migration and invasion. A, Expression of S100PBP, RhoA, RhoB, p-MYPT1-S^{696}, total MYPT1, p-cofilin-S^{3}, total cofilin and control GAPDH after transient silencing of S100PBP by specific siRNA mol1 (S100PBP mol1) and mol2 (S100PBP mol1) in Panc1 and MIA PaCa-2 cell lines. Control cells were transfected by non-target siRNA (scram). B, Cellular localisation of F-actin in the abovementioned cell lines. Arrows represent stress fibre formation. C, Increased rate of cell migration detected by time-lapsed microscopy after S100PBP silencing with siRNA mol2 in Panc1 and MIA PaCa-2 cells. Nuclei are stained by DAPI. D, Increased invasion of MIA PaCa-2 cells after silencing S100PBP (S100PBP mol2) detected by Matrigel invasion assay: representative Matrigel insert (top panel), number of invading cells (bottom panel).

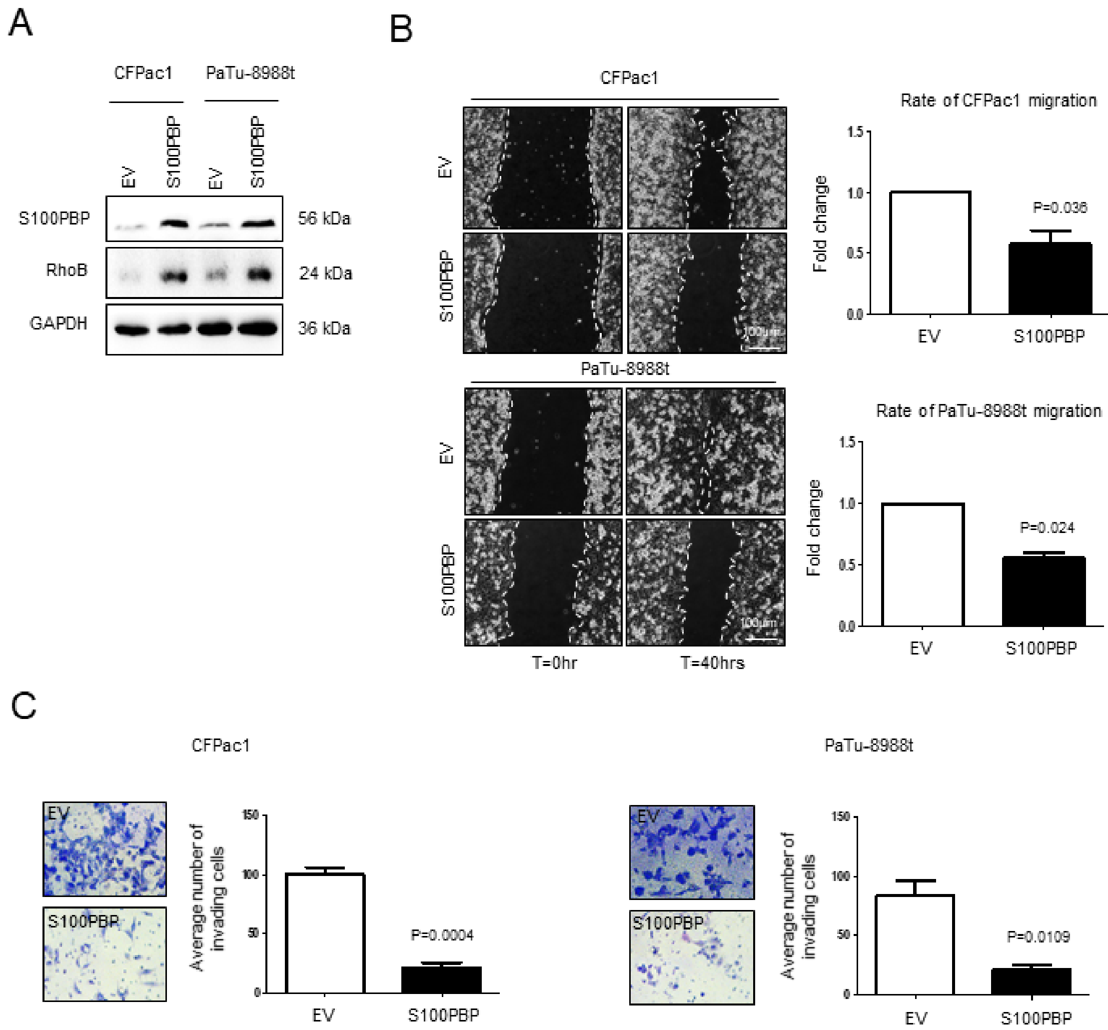

Figure 3

Stable overexpression of S100PBP attenuates cell migration and invasion. A, Levels of S100PBP and RhoB in CFPac1 and PaTu-8988t cells after stable expression of S100PBP. EV=cells transduced with empty vector. GAPDH was used as a loading control. B, C. Significant decrease in migration and invasion, respectively is shown.

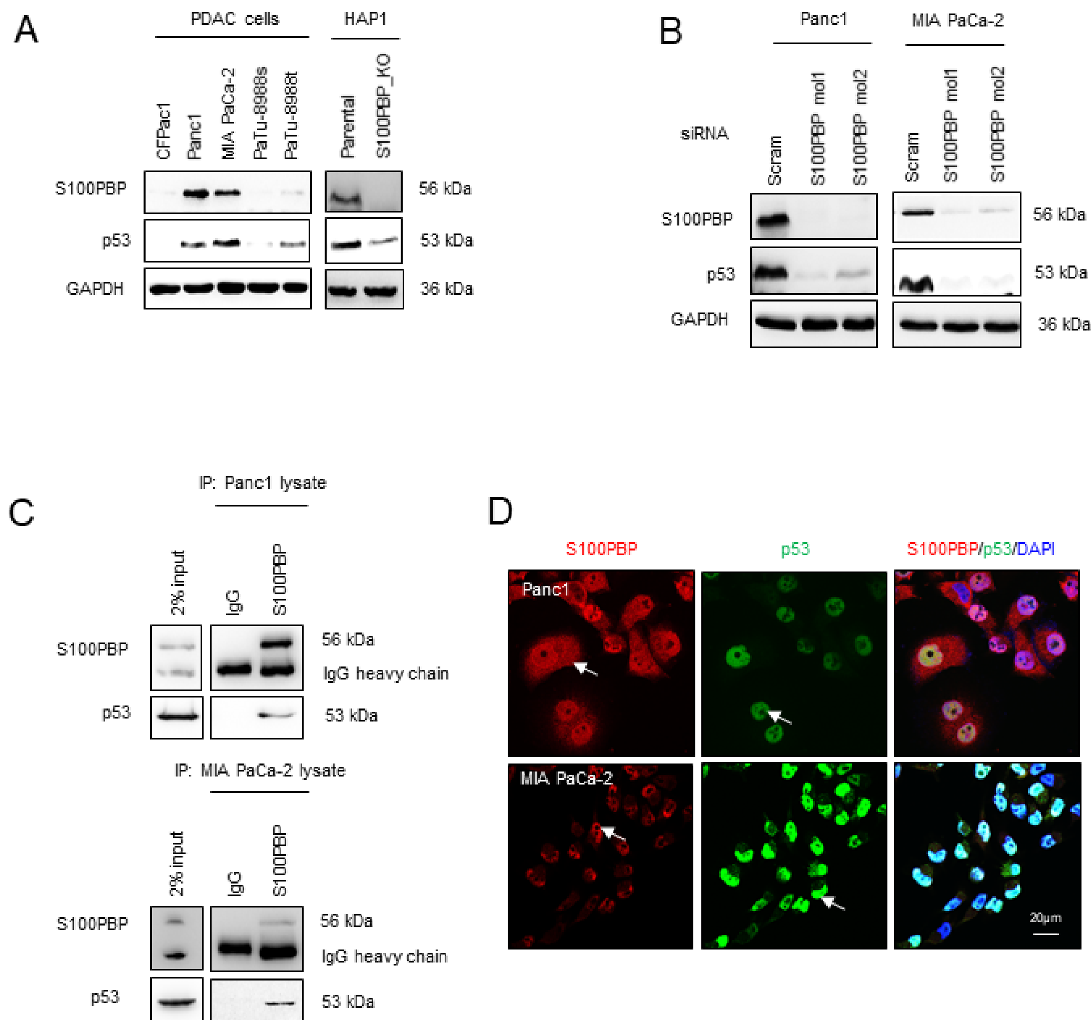

Figure 4

Interaction of p53 and S100PBP proteins. A, Expression of S100PBP and p53 in panel of PDAC cells and parental vs S100PBP_knock out (KO) HAP1 cells (parental vs S100PBP_knock out (KO)) before and B, after transient silencing by siRNA molecules (Scram, S100PBPmol1 and mol2) in Panc1 and MIA PaCa-2 cells. GAPDH was used as a loading control. C, Co-immunoprecipitation of S100PBP and p53 proteins in IP samples from Panc1 (top panel) and MIA PaCa-2 (bottom panel) lysates. Rabbit-IgG acted as internal

control; input sample was 2% of whole cell lysates. D, Cellular localisation of S100PBP and p53 in Panc1 and MIA PaCa-2 cells. Nuclei are stained by DAPI. Arrows represent sub-cellular localisation of respective proteins; the co-localisation of both proteins suggests that they interact in the nucleus.

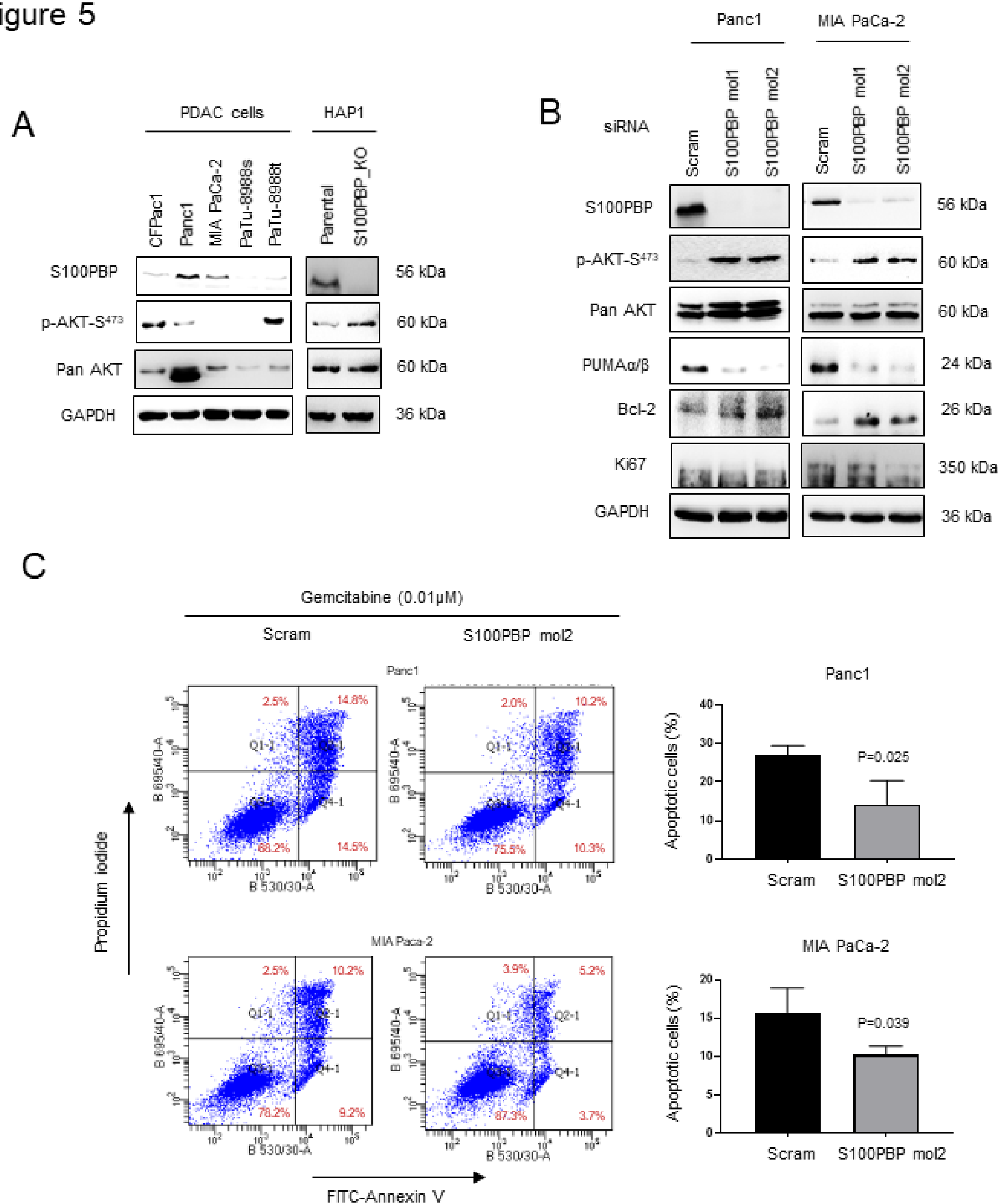

Figure 5

Inverse correlation between pro-survival AKT and S100PBP proteins. A, Expression of S100PBP, p-AKT-S^{473} and pan AKT in panel of PDAC and HAP1 cells (parental vs S100PBP_knock out (KO)) before and B, after transient silencing of S100PBP by specific siRNA mol1 and mol2 in Panc1 and MIA PaCa-2 cell lines. The differential protein expression of PUMAα/β and Bcl-2 are also shown. No changes in Ki67 were seen. GAPDH was used as a loading control. The scram (non-target) siRNA transfected cells were treated as respective controls. C, Increased percentage of apoptotic cells detected by FITC-Annexin V/Propidium iodide flow cytometry after S100PBP silencing (mol2) in Panc1 and MIA PaCa-2 cells followed by gemcitabine (0.01μM) treatment for 96 hours was observed.

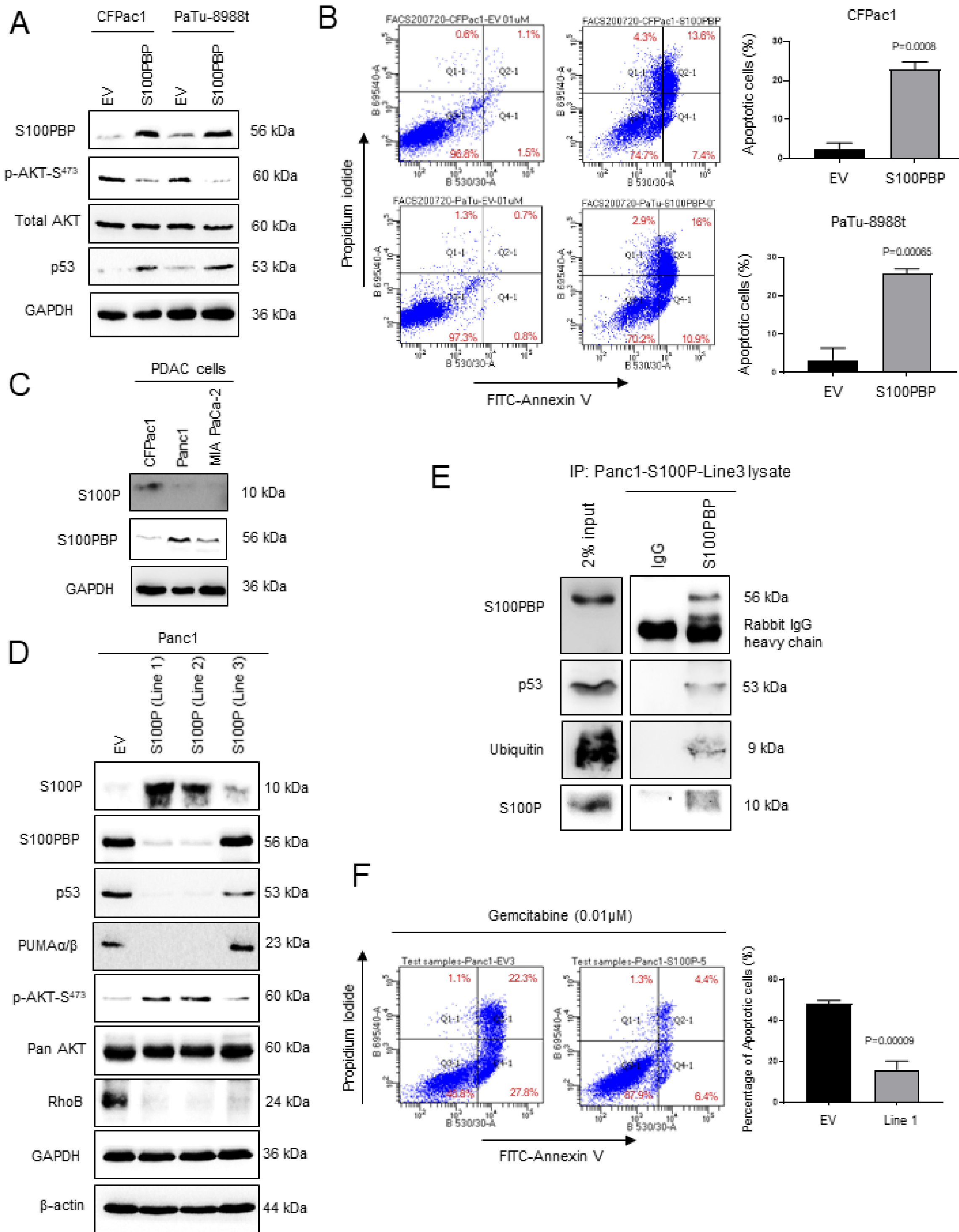

Figure 6

S100PBP attenuates cell survival, while S100P downregulates S100PBP and increases survival of cancer cells. A, Expression of S100PBP, p-AKT-S^{473}, pan AKT, and p53 in CFPac1 and PaTu-8988 cells stably expressing S100PBP protein. Cells transduced with empty vector (EV) were treated as respective controls. GAPDH was used as a loading control. B, Significant increase in percentage of apoptotic cells detected by FITC-Annexin V/Propidium iodide flow cytometry in stably expressing S100PBP cells after

gemcitabine (0.01μM) treatment for 96 hours is shown. C, Inverse expression of S100P and S100PBP in PDAC cell lines. GAPDH was used as a loading control. D, Expression of S100P, S100PBP, p53, PUMAα/β, p-AKT-S^{473}, pan AKT and RhoB in three Panc1 cell lines (Line 1, 2 and 3) after stable overexpression of S100P. Panc1 cells transduced with empty vector (EV) were used as controls. GAPDH and β-actin were loading controls. E, Immunoprecipitation (IP) of S100PBP protein and subsequent detection of p53, ubiquitin and S100P proteins in IP samples from Panc1-S100P Line3 lysates. Rabbit-IgG acted as internal control and input sample was 2% of whole cell lysates. F, Significant decrease in percentage of apoptotic cells detected by FITC-Annexin V/Propidium iodide flow cytometry in Panc1-S100P (Line1) cells after gemcitabine (0.01μM) treatment for 96 hours.

Figure 7

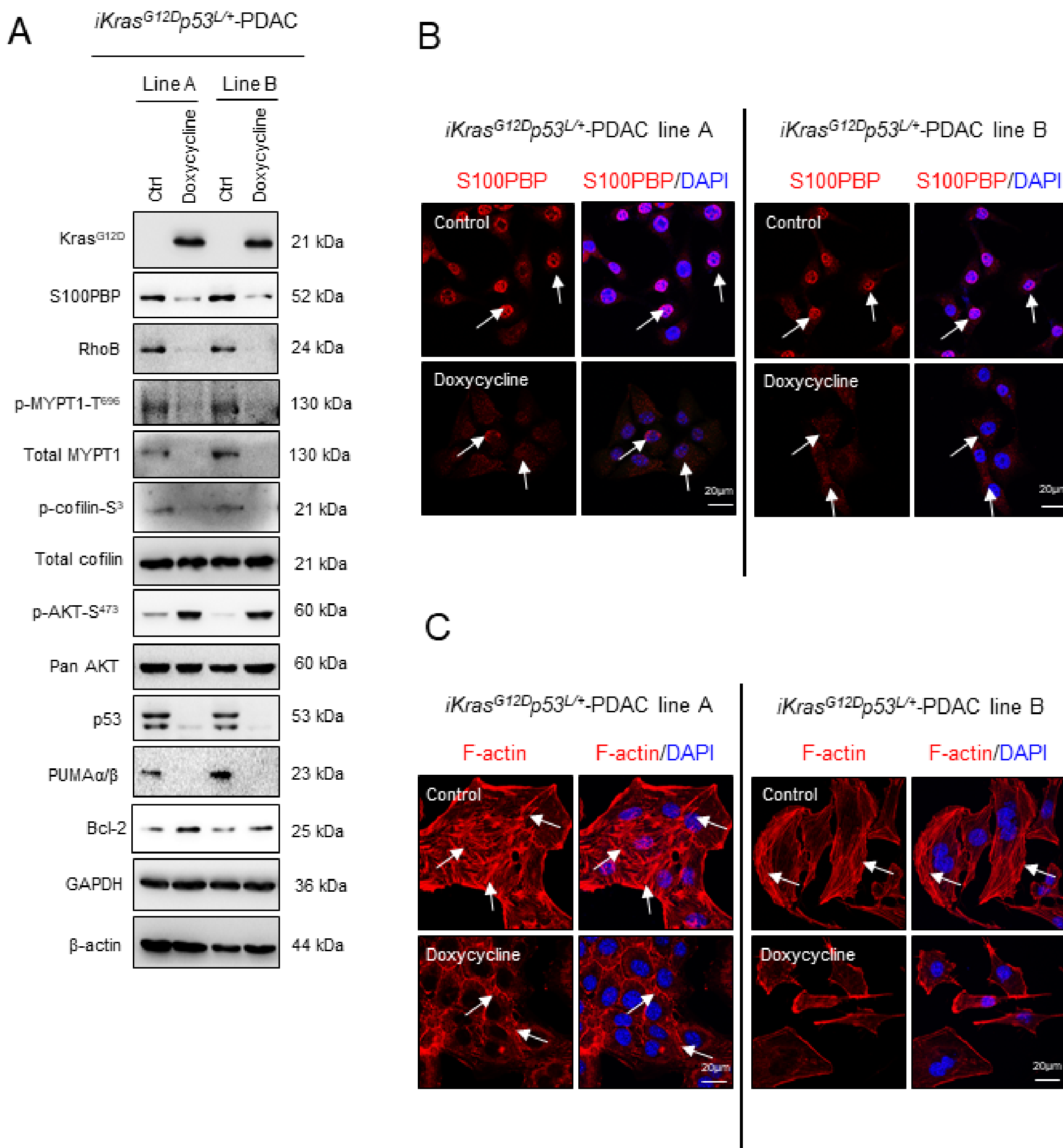

Figure 7

Kras^{G12D} activation downregulates S100PBP while activating AKT signalling. A, Differential expression of Kras^{G12D}, S100PBP, RhoB, p-MYPT1-S^{696}, total MYPT1, p-cofilin-S^{3}, total cofilin, p-AKT-S^{473}, pan AKT, p53, PUMAα/β and Bcl-2 proteins in two iKras mouse PDAC cell lines (A and B) after doxycycline (1μg/mL) treatment for 24 hours. GAPDH and β-actin were used as loading controls. B, Translocation of S100PBP (arrows) from nuclei (DAPI) in untreated (Control) iKras cells to the cytoplasm in Doxycycline treated

cells. C, Changes in F-actin in the abovementioned cell lines. Arrows represent thick cortical staining and stress fibre formation.

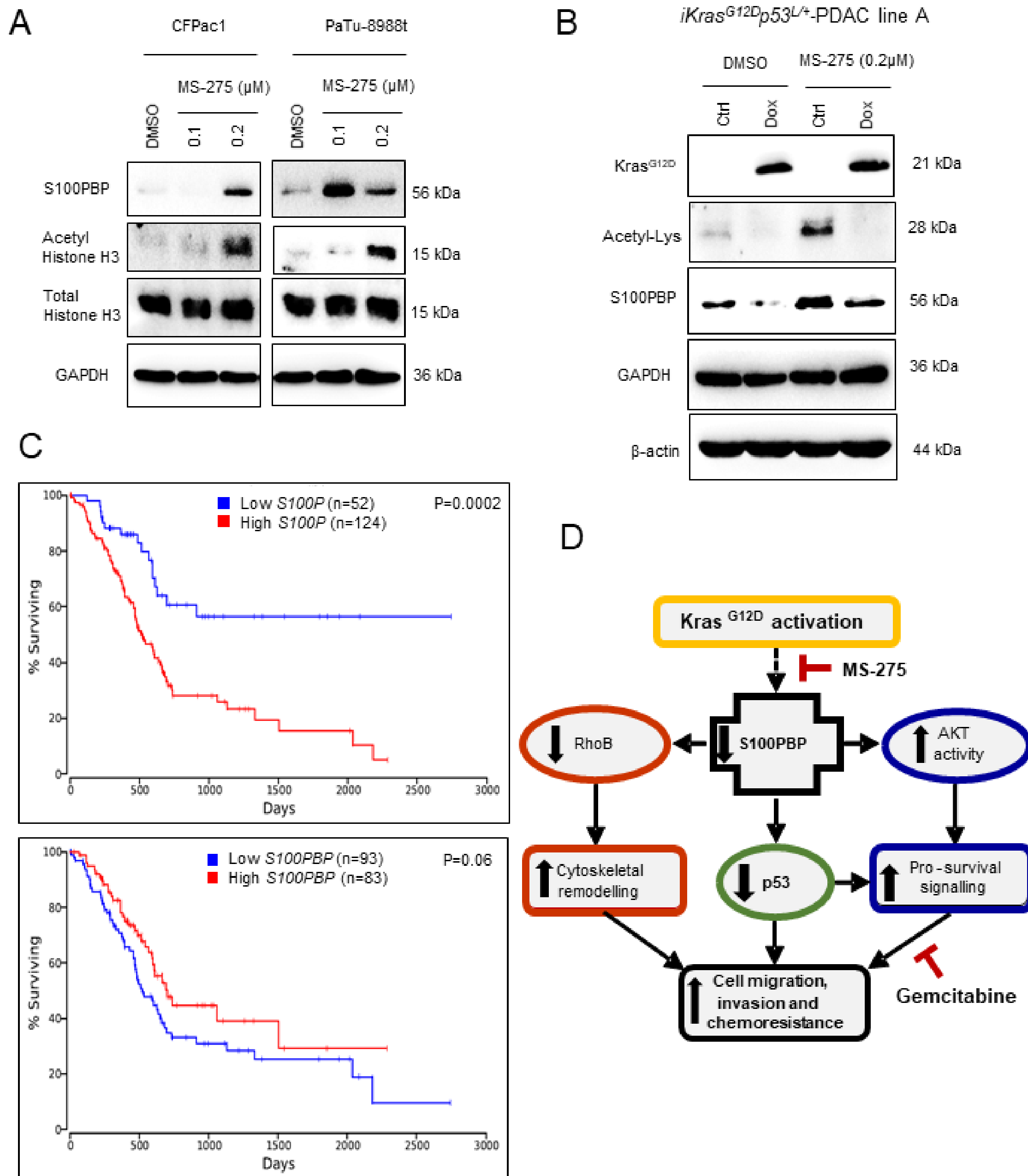

Figure 8

Inhibition of HDAC activity rescues S100PBP expression. A, Expression of S100PBP, Acetyl histone H3 and total histone H3 in CFPac1 and PaTu-8988t cell lysates after treatment with 0.1 or 0.2μM MS-275 or

DMSO vehicle for 72 hours shows rescued S100PBP expression in these cell lines. B, Expression of $Kras^{G12D}$, S100PBP and Acetyl-Lysine in iKras mouse PDAC cell lysates after 24 hours pre-treatment with 0.2μM MS-275 followed by treatment with doxycycline (1μg/mL) for further 24 hours to confirm the $Kras^{G12D}$-mediated epigenetic modification of S100PBP. GAPDH and β-actin were used as loading controls C, Kaplan-Meier survival plots using TCGA PanCancer Atlas dataset from 176 pancreatic adenocarcinoma patients. Patients with high S100P and low S100PBP expression had worse survival. D, Schematic representation of $Kras^{G12D}$/S100PBP signalling axes in PDAC cells.

Supplementary Files

This is a list of supplementary files associated with this preprint. Click to download.

- SupplementaryfiguresOncogene2023.pptx